A Signal Processing System for Extraction of Harmonics and Reactive Current of Single-Phase Systems

Masoud Karimi-Ghartemani, Hossein Mokhtari, M. Reza Iravani, *Fellow, IEEE*, and Mohammad Sedighy, *Member, IEEE*

***Abstract*—A signal processing system for extraction of harmonic and reactive current components is introduced and its performance is evaluated. The extraction system is adopted as part of the control system of a single-phase active power filter (APF) to provide the required signals for harmonic filtering and reactive power compensation. Performance of the overall system is evaluated based on digital time-domain simulation studies. The APF control system including the signal processing algorithms are implemented in Matlab/Simulink Fixed-Point Blockset to accommodate bit-length limitation which is a crucial factor in digital implementation. The power system including the APF, load and the supply system are simulated with the PSCAD/EMTDC software to which the Matlab-based control model is interfaced. The simulation results indicate that the signal processing unit can provide the required signals for APF to perform filtering/compensation within the transient period of 2 to 3 cycles.**

***Index Terms*—APF, FACTS, harmonics, power factor adjustment, reactive current, STATCOM.**

I. Introduction

ACTIVE compensation of harmonics, reactive power and unbalance is required for improving power quality, control and protection [1]–[3]. An integral part of an active compensation device is the detection unit which generates the reference signals. Various methods, e.g. Discrete Fourier Transform (DFT), Phase-Locked Loop (PLL), notch filtering and theory of instantaneous reactive power have been presented in the literature for this purpose [4]–[9].

This paper introduces a single-phase signal processing system for extraction of harmonic and reactive current components for use in FACTS and Custom Power Controllers, e.g. Active Power Filters (APFs), Unified Power Flow Controllers (UPFCs) and STATic Var COMpensators (STATCOMs). The system is based on an enhanced phase-locked loop (EPLL) system and its features with respect to other methods are as follows.

- It simultaneously extracts harmonic and reactive current components independently.
- Its structure is adaptive with respect to frequency.
- Its structure is robust with respect to the setting of the internal parameters.
- Its performance is immune to noise and external distortions.
- Accuracy and speed of its response are controllable.
- Its structural simplicity provides major advantage for its implementation within embedded controllers.

This paper is also to evaluate the performance of the EPLL-based system for a single-phase APF application for harmonic filtering and reactive power compensation. The EPLL-based system is implemented in the Fixed-Point Blockset of Matlab [10]. This takes into account the impact of bit-length which is important for digital implementation of the algorithm. The power system of the APF is simulated in the PSCAD/EMTDC [11] environment to which the Matlab/Simulink model of the EPLL-based system is interfaced through a software link.

The paper is organized as follows. The structure of the EPLL-based system for extraction of harmonic and reactive current components is described in Section II. Section III establishes the criteria to derive the required reference signals for achieving the desired level of harmonic elimination and power factor correction. Independent performance of the proposed EPLL-based system is studied in Section IV. Performance of the EPLL-based system when adopted for a single-phase APF system is studied and discussed in detail in Section V. Section VI concludes the paper.

II. EPLL-Based System

A. EPPL

A block diagram of the EPLL is shown in Fig. 1 [12]. As conventional PLL, EPLL is comprised of three blocks of phase detector (PD), loop filter (LF) and voltage-controlled oscillator (VCO). The EPLL receives the input signal $u(t)$ and provides an on-line estimate of the following signals:

- The synchronized fundamental component, $y(t)$.
- The amplitude, $A(t)$, of $y(t)$.
- The phase angle, $\phi(t)$, of $y(t)$.
- The frequency deviation, $\Delta\omega(t) = \omega(t) - \omega_o$.
- Time-derivatives of the amplitude, phase and frequency.

The error signal, $e(t) = u(t) - y(t)$, is the total distortion signal of the input. Stability of the EPLL system is analyzed in [13] and shown that the speed of response is determined by

Manuscript received February 28, 2003. Paper No. TPWRD-00450–2002.

M. Karimi-Ghartemani and M. R. Iravani are with the Centre for Applied Power Electronics (CAPE), Department of Electrical and Computer Engineering, University of Toronto, Toronto, ON M5S 3G4, Canada (e-mail: masoud@ele.utoronto.ca; iravani@ecf.utoronto.ca).

H. Mokhtari is with the Department of Electrical and Computer Engineering, Sharif University, Tehran 11365-8639, Iran (e-mail: mokhtari@sharif.edu).

M. Sedighy is with Hatch Associates Ltd., Mississauga, ON L5K 2R7, Canada (e-mail: msedighy@hatch.ca).

Digital Object Identifier 10.1109/TPWRD.2004.829942

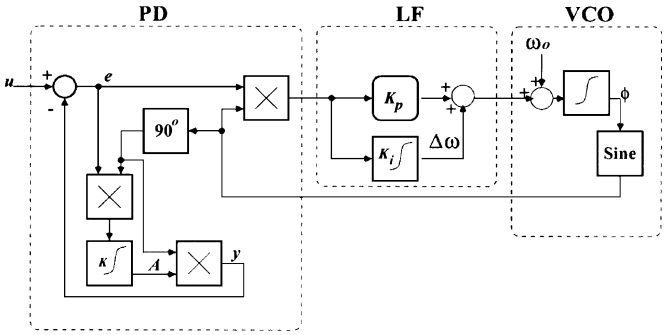

Fig. 1. Block diagram of the EPLL.

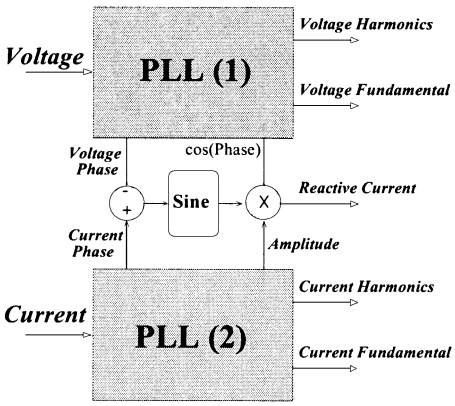

Fig. 2. Block diagram of the proposed single-phase harmonic/reactive-current extraction unit employing two units of the EPLL.

parameters K, K_p and K_i. These parameters control transient as well as steady-state behavior of the response.

The EPLL is inherently adaptive and follows variations in amplitude, phase angle and frequency of the input signal. The EPLL is capable of accurately estimating the fundamental component of a polluted signal. The structure of the EPLL is simple and this makes it suitable for real-time embedded applications for software or hardware implementation.

Another feature of the EPLL is its ease of tuning which is accomplished by assignment of the parameters. A range of values for these parameters are valid for any particular application at hand; i.e. the structure is insensitive with respect to variations in the internal parameters. This insensitivity to internal parameters and its insensitivity with regard to characteristics of the external input signal and noise constitutes the robustness of the EPLL.

B. Single-Phase Harmonic/Reactive-Current Extraction

This section explains the structure of a single-phase harmonic and reactive-current extractor unit based on the EPLL described in the preceding section. The proposed unit, although is intended for extracting harmonic and reactive current components, also extracts other pieces of information such as peak value, phase angle and frequency of the fundamental component, Total Harmonic Distortion (THD), and power factor.

Assume $v(t) = v^f(t) + v^h(t)$ is the distorted load voltage and

$$v^f(t) = V_1 \sin(\phi_v) \tag{1}$$

is its fundamental component extracted by employing an EPLL. Thus, the total harmonic content and the amplitude, phase angle and frequency of the fundamental component are also extracted and made available.

Let $i(t) = i^f(t) + i^h(t)$ denote the distorted load current where

$$i^f(t) = I_1 \sin(\phi_i) \tag{2}$$

represents its fundamental component which is extracted by another EPLL unit. Signal $i^h(t)$ represents the total distortions of the current signal. The amplitude and phase angle of the fundamental component of the current signal are also made available at the outputs of the unit.

The fundamental component $i^f(t)$ of the current signal $i(t)$ can be written as

$$i^f(t) = I_1 \sin(\phi_i) = i_a^f(t) + i_r^f(t) \tag{3}$$

where $i_a^f(t)$ and $i_r^f(t)$ represent active and reactive components of $i^f(t)$ and expressed as

$$i_a^f(t) = I_1 \cos(\phi_i - \phi_v) \sin(\phi_v) \tag{4}$$

$$i_r^f(t) = I_1 \sin(\phi_i - \phi_v) \cos(\phi_v). \tag{5}$$

It is noteworthy that I_1, ϕ_v, ϕ_i, $\cos\phi_v$, and $\sin\phi_v$ are all made available by the two EPLLs and the additional calculations needed are: a subtraction to produce $\phi_i - \phi_v$, a sine function and two multiplications.

Fig. 2 shows a block diagram of the single-phase harmonic/reactive-current component extractor. Two identical EPLL units are used for voltage and current signals. The top portion of the unit is used for voltage and the bottom portion is used for current signal processing. The link between the two parts is to calculate the fundamental reactive current component. This structure also provides harmonic content of voltage, $v^h(t)$, peak values of both voltage and current fundamental components, A_v and A_i, their phase angles ϕ_v and ϕ_i, and the phase angle between voltage and current signals.

C. THD Calculation

The THD calculation of the input signal (being voltage or current) can be computed using the outputs of the corresponding EPLL. Let $x(t)$ be the input signal to the EPLL and $x^f(t)$, $x^h(t)$, A_x, and ϕ_x be the outputs of the EPLL corresponding to the fundamental component, harmonic content, amplitude and phase angle. By definition, the THD of $x(t)$ is

$$THD_x = \frac{\sqrt{\frac{1}{T_o}\int_{T_o} [x^h(t)]^2\, dt}}{A_x \sqrt{\frac{1}{2}}} \times 100\% \tag{6}$$

in which the numerator is the square root of the dc value of $[x^h(t)]^2$ which can be provided by a Low-Pass Filter (LPF), and $f_o = (1/T_o)$ is the input center frequency.

Fig. 3 shows the structure to implement the THD calculating unit based on (6). The LPF is of first-order with the transfer function $H(s) = (2)/(1 + \tau s)$. The gain 2 is to implement the $\sqrt{1/2}$ in the denominator of (6). The smaller the value of $\tau > 0$ is chosen, the smoother and more precise the THD is computed, but in a longer duration of time. A suggested value is $\tau = (1/2\pi 20)$ (s/rad).

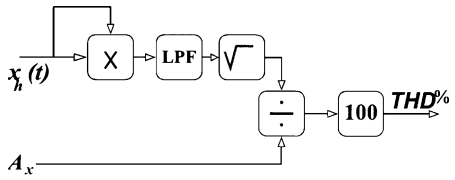

Fig. 3. Block diagram of the THD calculating unit.

D. Setting of the Parameters

Parameters K, K_p and K_i determine the speed of convergence of the EPLL toward its solution in terms of amplitude, phase and frequency. The dynamics of the variables are coupled and they mutually effect each other. The convergence rate increases with the increase in the values of the parameters. However, an increase in a parameter value results in a larger steady-state error or a misadjustment in the estimated values in the presence of noise and distortions. This effect, which is an inherent feature of an adaptive algorithm, necessitates trade-off according to the desired dynamic and steady-state responses.

Theoretical studies in [12] show that the time-constants of the linearized system are $\tau_1 = 2/K$ and $\tau_2 = (2/K_pA_o)$ corresponding to the amplitude and phase angle, respectively. For a one p.u., 50 Hz, input signal, the values of $K = K_p = 200$ would result in a convergence rate of around two to three cycles which is appropriate for most power system applications. Larger values for these parameters result in a larger steady-state error, specially in cases where the input has a high pollution content. With a small input pollution content, one can increase these parameters and yield faster convergence without introducing significant steady-state errors.

E. Performance Improvement

As mentioned before, increasing a parameter value increases the rate of convergence of the corresponding variable, Fig. 1, nevertheless a higher level of steady-state error is introduced. This error manifests itself as a small oscillations around the value of the corresponding variable. It is possible to reduce the error by low-pass filters (LPFs). These filters should be placed one after the integration unit in the PD, which estimates the amplitude, and the other in the LF, which estimates the phase angle, Fig. 1. Our observations indicate that a first-order LPF, with a cut-off frequency of about 30 Hz, suppresses the error considerably and permits the parameters to be increased to obtain a speed of response twice as high as the original structure with the same level of error. These LPFs also increase robustness with respect to high frequency disturbances and noise since the amplitude, phase angle and frequency of the fundamental component are more smoothly estimated.

Fig. 4 shows an alternative system for extraction of harmonic and reactive current components using one single unit of EPLL. The limitation of the system of Fig. 4, compared to that of Fig. 2, is that it extracts the sum of harmonic and reactive current components rather than extracting them separately. Moreover, this structure does not provide some of the helpful information, e.g. amplitudes and phase angles, which are provided by the structure of Fig. 2. This structure is included here for the sake of completeness and to provide comparison with an analogous method presented in [6]. Principles of operation of the system of Fig. 4 are briefly explained as follows.

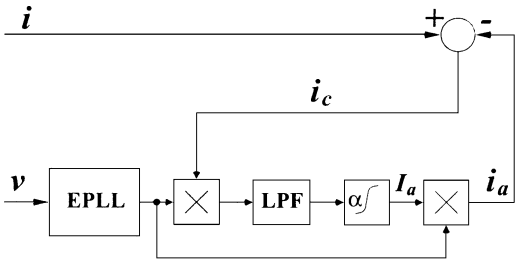

Fig. 4. Extracting sum of harmonic and reactive current components.

The current signal $i(t)$ is comprised of an active component, $i_a^f(t)$, a reactive component, $i_r^f(t)$, and distortion component $i^h(t)$. $i_a^f(t)$ is in-phase with the voltage fundamental component. An EPLL unit is employed to extract a normalized sinusoid which is in-phase with the voltage fundamental component, Fig. 4. This signal is then used in a feedback control loop to estimate the amplitude of the active current component, I_a. Multiplication of this amplitude with the sinusoid yields $i_a^f(t)$. Subtraction of $i_a^f(t)$ from the current signal results in the sum of harmonic and reactive current components $i_c = i - i_a^f = i_r^f + i^h$.

The feedback loop is the standard loop of adaptive algorithms. The LPF is a first-order, low-pass filter with a bandwidth of about 20 Hz for an integrating gain of $\alpha = 100$. Larger values of the bandwidth and α increase the estimation speed while introduce higher level of steady-state error.

The system of Fig. 4 is analogous to the frequency-independent method of [6] in which a conventional PLL system is employed. Performance of the method of [6] for a wide range of frequencies without extra tuning stages is reported in [6]. Compared to that of [6], the system of Fig. 4 provides the same level of performance for even a wider range of frequencies without any readjustment of the parameters. An additional feature of the system of Fig. 4 as compared to the system of [6] is its ability to estimate the voltage fundamental component, amplitude, phase angle and frequency.

III. Reference Signals

In this section, the appropriate reference signals to achieve a desired level of harmonic elimination and power factor correction by a single-phase active filter are specified. Assume that $v(t)$ and $i(t)$ represent the single-phase load voltage and current signals. Both v and i in general are nonideal and distorted.

A. Harmonic Elimination

If $i(t)$ is fed to the EPLL system, the fundamental component $i^f(t)$ and the total sum of all harmonics $i^h(t)$ are extracted. To eliminate $H\%$ of this harmonic signal from the load current, an APF must inject

$$i_c^h(H,t) = 0.01Hi^h(t), \tag{7}$$

where the subscript c is for compensation. Note that this will eliminate $H\%$ of the total harmonic signal with no specific levels of compensation for individual harmonic components. The THD of the signals is also computed by the EPLL-based system and provides an index to judge the level of harmonic compensation by an APF. The relation between the initial THD

(before filtering), the obtained $\mathrm{THD}^{\mathrm{new}}$ (after filtering $H\%$) and H is $\mathrm{THD}^{\mathrm{new}} = (100 - H)\mathrm{THD}$.

B. Power Factor Correction

Suppose the power factor of the system, calculated by the detection unit, is PF which corresponds to a fundamental reactive current component of $i_r^f(t)$. To compensate $Q\%$ of this reactive component and correct the power factor to the new value PF^{new}, a total current of

$$i_c^r(Q,t) = 0.01Qi_r^f(t) \tag{8}$$

should be injected. The relationship between Q and PF^{new} is expressed by

$$PF^{\mathrm{new}} = \frac{PF}{\sqrt{PF^2 + (0.01Q-1)^2(1-PF^2)}}. \tag{9}$$

As Q varies from zero to 100, PF^{new} varies from its old value, i.e. PF, to unity.

The proposed system of Fig. 2 provides separate extraction of harmonic and reactive current components and an APF system that is based on this method is furnished with independent compensation of harmonic and reactive current components. The system of Fig. 4 and also the method of [6] provide sum of harmonic and reactive current components and, thus, independent compensation of these two components is not possible.

IV. Stand-Alone Performance of the EPLL-Based System

Simulated performance of the detection unit is presented in this section. MATLAB and SIMULINK software tools are used for the simulation studies.

A. Harmonics

1) Dynamic Initiatory Performance: An input signal comprising 1 p.u. of the fundamental component, 1/3 p.u. of the third harmonic and 0.2 p.u. of the fifth harmonic is considered for the simulation. The outputs of the single-phase EPLL-based extraction system are presented in Fig. 5. The extracted fundamental component including its amplitude, extracted harmonics, and error are shown in parts (a), (b), and (c), respectively. The error signal shown in part (c) is the error in the harmonic signal (or equivalently in the fundamental component). It is observed that the transient stage (initialized at zero values) is completed in about two cycles.

2) Steady-State Performance: Fig. 6 shows continuation of Fig. 5 from 100 ms to 200 ms to illustrate the steady-state response. A maximum steady-state error of 1% is observed for the highly polluted input signal $(\mathrm{THD} = 39\%)$.

B. Reactive Current Component

Performance of the EPLL-based system in extracting the reactive current component is shown in Fig. 7. The ideal input voltage and current signals are in phase up to $\mathrm{t} = 20\ \mathrm{ms}$ and hence no reactive component exists. At $\mathrm{t} = 20\ \mathrm{ms}$, the voltage signal is shifted by $(\pi/2)\ \mathrm{rad}$. Fig. 7(a) shows the extracted reactive current component. Fig. 7(b) shows the detected phase difference between the voltage and current signals. The reactive

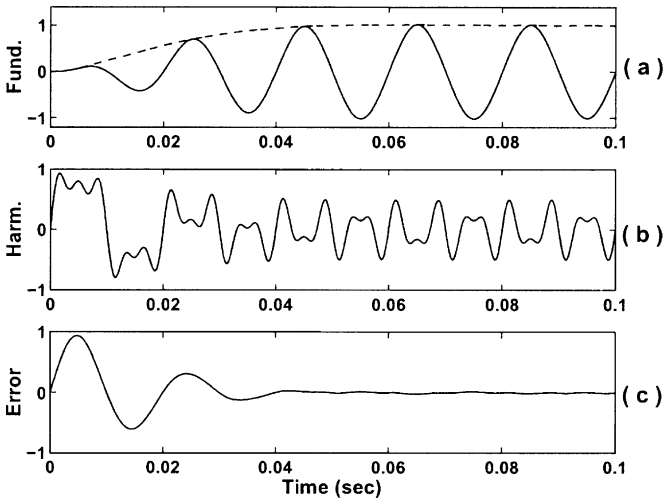

Fig. 5. Dynamic performance of the EPLL-based system for an input signal comprising of 1 p.u. of the fundamental component, 1/3 p.u. of the third harmonic and 0.2 p.u. of the fifth harmonic $(\mathrm{THD} = 39\%)$: (a) extracted fundamental component and its amplitude, (b) extracted harmonic signal, and (c) error.

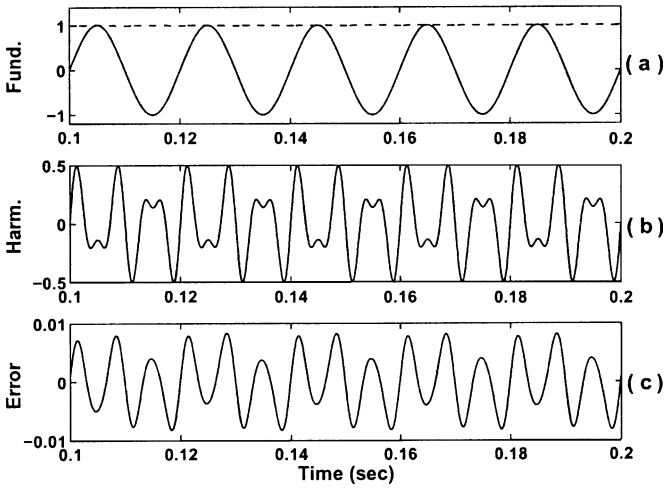

Fig. 6. Steady-state performance of the EPLL-based system: continuation of the graph of Fig. 5 over the period of 0.1 to 0.2 seconds.

current component has been accurately detected within almost one cycle.

Performance of the alternative system of Fig. 4 is also evaluated by the following example. The current signal is a square wave signal whose amplitude and phase angle undergo a 50% jump and a 45 degrees shift at $\mathrm{t} = 0.04$ and $\mathrm{t} = 0.12\ \mathrm{s}$ respectively, as shown in Fig. 8(a). The voltage signal is comprised of the fundamental component and 10% of the seventh harmonic. The extracted active current component and the sum of harmonic and reactive current components are shown in Fig. 8(b) and (c), respectively. The accuracy and the transient response time are the same as that of the method presented in [6].

V. Performance of the EPLL-Based Signal Extraction System in an APF System

In this section, the EPLL-based system is employed as part of the control system of a single-phase APF and performance of the overall system, in the context of harmonic and reactive

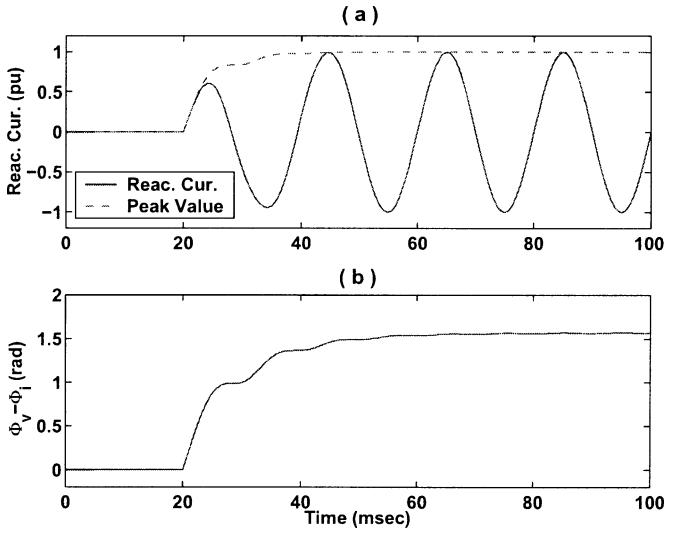

Fig. 7. Reactive current detection by the EPLL-based system for a step change of $\pi/2$ (rad) in the phase angle: (a) reactive current component and its peak value (b) phase difference.

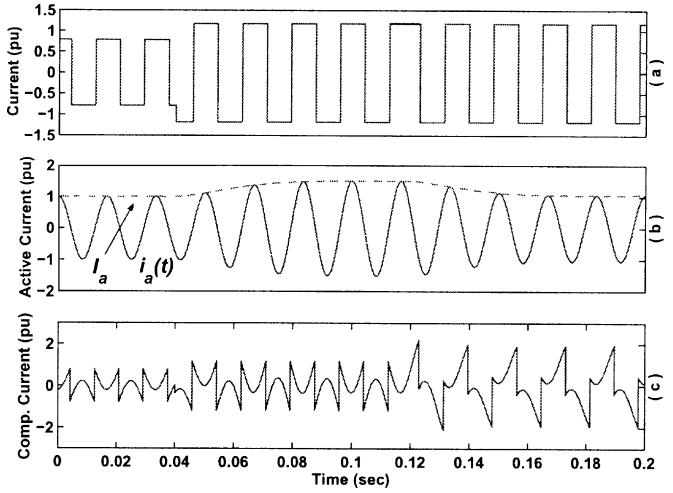

Fig. 8. Performance of the structure of Fig. 4(a) current signal whose amplitude and phase angle undergo a 50% jump and a 45 degrees shift at $t = 0.04$ and $t = 0.12$ sec, respectively (b) extracted active component of the current and its amplitude (c) extracted sum of harmonic and reactive current components.

power compensation, is evaluated. The EPLL-based system is simulated using MATLAB Fixed-Point Blockset [10] to accommodate word-length limitation effects. This represents a digital fixed-point implementation platform such as an Field Programmable Gate Arrays (FPGA). The APF power system is simulated using the EMTDC/PSCAD [11] software package. The MATLAB Fixed-Point Blockset and the EMTDC/PSCAD are interfaced [11] to provide dynamic simulation of the power circuitry and the detection/control of the overall APF system.

A. Active Power Filter

The structure of the APF is shown in Fig. 9 [15]. The APF is designed to compensate harmonic and reactive current components in the single-phase line that connects the supply system to the load, Fig. 9. The power system consists of:

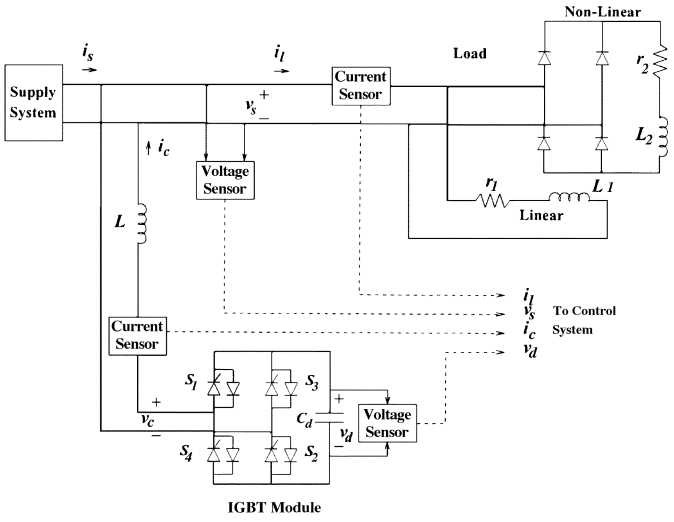

Fig. 9. Power circuit of the active power filter.

- AC power source with the following parameters:
  - rated voltage: 115 V
  - rated frequency: 60 Hz
  - internal inductance: 80 μH
- load is composed of:
  - a linear RL with $r_1 = 7.5\,\Omega$ and $L_1 = 43$ mH
  - a single-phase full-bridge rectifier with the dc-side load of: $r_2 = 4.9\,\Omega$ and $L_2 = 200$ mH, (ideal switches assumed)
- a full bridge voltage-source converter (VSC) APF with the following parameters:
  - DC capacitance C_d: 4800 μF
  - filter inductance L: 2.5 mH
  - switching frequency: 8192 Hz
  - average DC Voltage: 220 V
  - (ideal switches assumed).

The load current i_l (Fig. 9) contains a fundamental component which lags the fundamental of the input voltage v_s by angle ϕ_1. It also contains harmonic components i_l^h. The function of the APF is to provide a current, i.e. i_c, which compensates for the load current harmonics and reactive current component. Therefore, the source current i_s will be harmonic free and in-phase with the load voltage v_s. In practice, the objective is to keep the THD of the source current within the recommended limit [14] and increase power factor to unity at the point of common coupling (PCC) by the APF.

1) Control System: The control system of the APF provides a switching pattern for the VSC such that the converter current can compensate for the prespecified levels of harmonics and reactive power. The control system is composed of a detection block, current control and voltage control units. Fig. 10 shows a block diagram of the control system [15].

2) Detection Block: The detection block, as a complementary part of the control system, extracts the harmonic and reactive current components to create a reference signal. This part of the control logic is performed by the EPLL-based system.

3) Current Control: The current control logic is based on the fact that the PCC voltage plus the voltage drops along the path

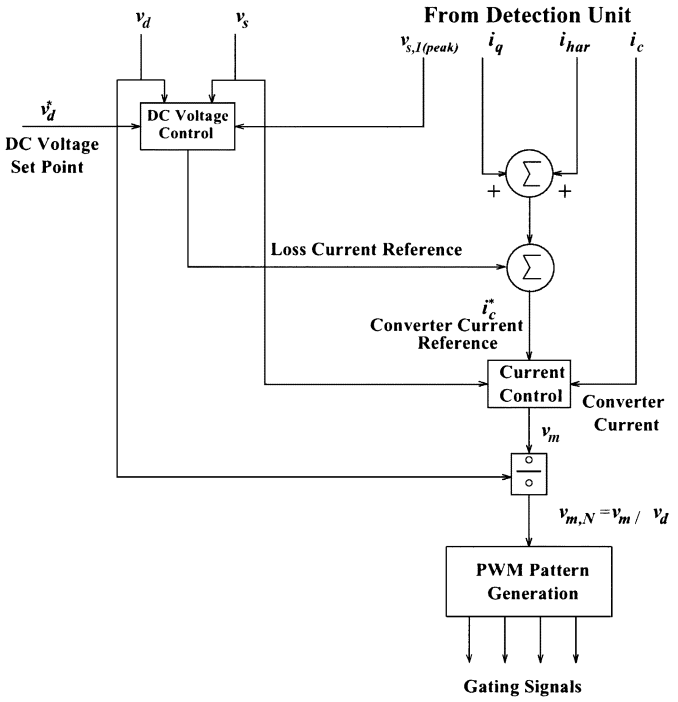

Fig. 10. Block diagram of the APF control system.

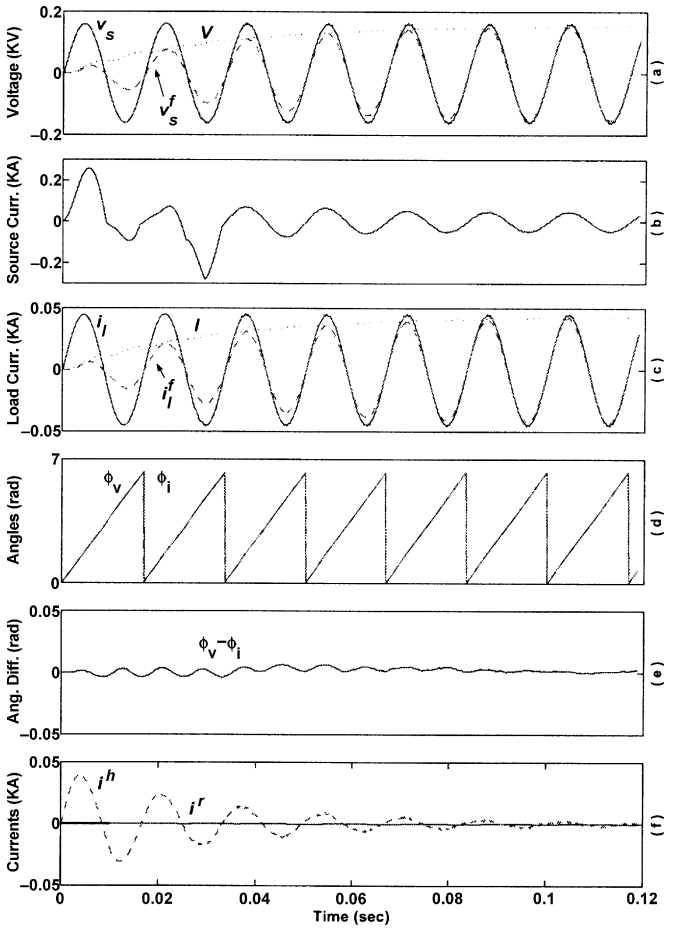

Fig. 11. APF performance with a pure resistive linear load: (a) PCC voltage (v_s), its extracted fundamental component (v_s^f) and amplitude (V) (b) source current (c) load current (i_l), its extracted fundamental component (i_l^f) and amplitude (I)(d) extracted phase angles of the voltage (ϕ_v) and current (ϕ_i) (e) their difference $(\phi_v - \phi_i)$ (f) extracted harmonics i^h and reactive current i^r.

from PCC to the VSC is equal to the converter voltage. Therefore, calculating the PCC voltage and the desired converter current, the converter voltage can be computed. The Pulse Width Modulation (PWM) pattern is generated such that the converter output voltage follows its reference. In summary, the current controller is composed of a voltage drop calculator plus a feed forward signal. Details of the current control logic are given in [15].

4) DC Voltage Control: The DC voltage control unit is to keep the DC voltage of the VSC constant at a predefined value. Thus, a fundamental frequency current reference is generated which is composed of two terms.

1) The first term of the current reference is due to the loss in the APF. To find the loss term, the mean square value of the load compensation current is obtained. An estimation of the APF loss is deduced based on the current and the estimated APF resistance. One can then calculate the current needed for loss compensation.
2) The second term of the current reference is due to the difference between the DC voltage and its reference. In this section, the mean square of DC voltage is compared to the mean square of the DC reference. The result, which is proportional to the difference between the desired and the actual energy of the capacitor, is divided by half of the peak fundamental voltage after passing through a gain controller [15].

The fundamental frequency current reference is then compared to a prespecified limit to prevent over current conditions. The current is synchronized with the input voltage prior to the PWM generator unit.

5) PWM Pattern Generator: Unipolar switching pattern has been used for the PWM generator of the VSC. In this mode of switching, the switches in each leg of the VSC are controlled independently.

B. Study Results

This section presents the simulation results of the APF system in which the detection part of the control logic is represented by the EPLL-based system. The results show both transient and steady-state behaviors of the overall system.

1) Resistive Load: All initial conditions of the detection algorithm are set to zero and the combination of the load and APF is energized at $\mathrm{t} = 0$. The load is assumed to be the pure resistive load r_1, Fig. 9. Fig. 11(a) shows the PCC voltage (v_s), its extracted fundamental component (v_s^f) and amplitude (V). The transient behavior in the source current, Fig. 11(b), is due to (1) the charging current of the VSC capacitor and (2) the transient stage in the detection of the harmonic content of the load current. The transient behavior is over when both the capacitor is fully charged and the detection algorithm reaches its steady state. Fig. 11(c) shows the load current (i_l), its extracted fundamental component (i_l^f) and amplitude (I). Parts (d), (e) and (f) of Fig. 11 show the phase angles, their difference, harmonic content of the current and reactive current component,

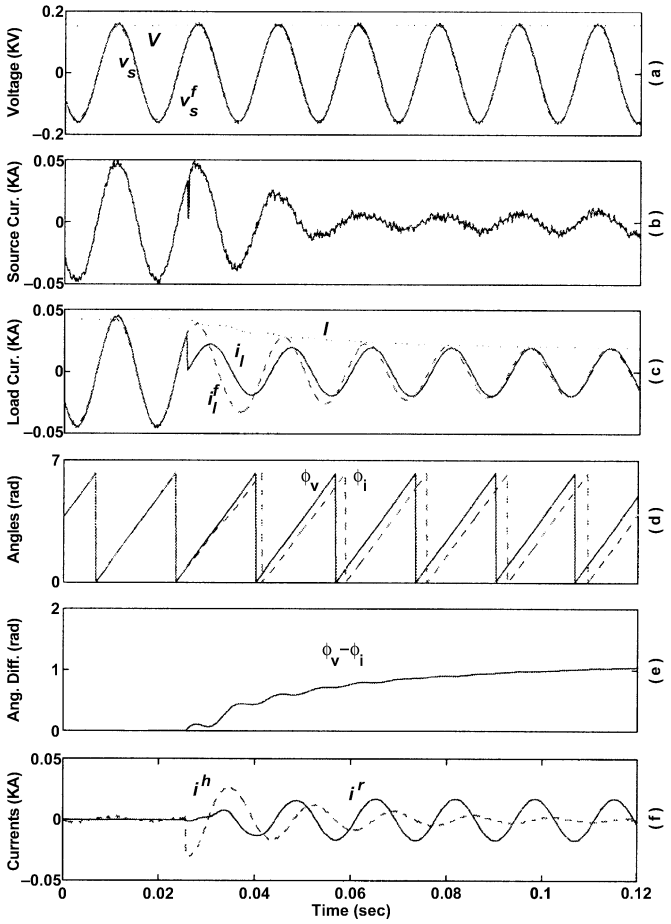

Fig. 12. APF performance when the pure resistive load is changed to an RL load at $\mathrm{t} = 0.024$ s: (a)–(f) as described in Fig. 11.

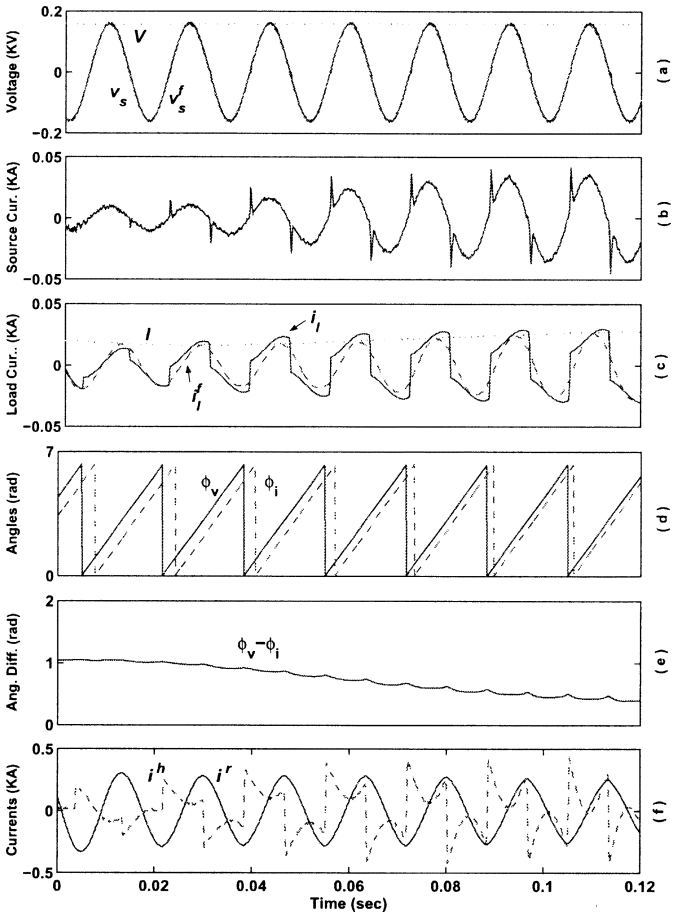

Fig. 13. APF performance when a nonlinear load is added to the RL load at $\mathrm{t} = 0.004$ sec: (a) to (f) as described in Fig. 12.

respectively. Detected harmonics and reactive currents components approach zero in the steady state. The transient time is about 3 cycles which is slower than the FFT-based method [15]. However, frequency-adaptivity and structural-simplicity and robustness are the features of the proposed method compared with the FFT-based methods.

2) Resistive+Inductive Load: This case studies closed-loop performance of the system when the resistive load is changed to a resistive plus inductive load. The system is initially in a steady-state with the resistive load r_1 is in service, when the inductive load L_1, Fig. 9, is switched in at $\mathrm{t} = 0.024$ s. PCC voltage (v_s), its extracted fundamental component (v_s^f) and amplitude (V) are depicted in Fig. 12(a). Source current is shown in Fig. 12(b) which settles to a sinusoidal form in-phase with the PCC voltage through proper reactive power injection by the APF. Load current (i_l), its extracted fundamental component (i_l^f) and amplitude (I) are shown in Fig. 12(c). Estimated phase angles of the voltage (ϕ_v) and current (ϕ_i) and their difference are shown in Fig. 12(d) and (e), respectively. The phase difference approaches a value of about one radian in the steady-state. Part (f) shows the harmonics and reactive current components extracted by the detection unit and compensated by the APF. No harmonic component exists in the steady state but a reactive current component with the amplitude of about 20 A exists due to the inductive part of the load. Transient time in the reactive current compensation is less than two cycles. The transient time is due to the (1) transient in the load and (2) transient response of the detection unit. The overall transient time is longer than the FFT method [15] but shorter than that of [6].

3) Nonlinear Load: Initially the RL load of previous section is in service under a steady-state condition. At $\mathrm{t} = 0.004\ s$ the rectifier load is connected to the system. Fig. 13(a) shows the PCC voltage. The source current remains sinusoidal and in-phase with the PCC voltage due to the harmonic filtering and reactive power compensation of the APF [Fig. 13(b)]. The load current, its extracted fundamental component and amplitude are shown in Fig. 13(c). Estimated phase angles and their difference are shown in Fig. 13(d)–(e). This difference approaches a value of about 0.4 radians from its original value of one radian. The extracted harmonic and reactive current components are shown in Fig. 13(f). Compensation of the harmonic and the reactive current components is achieved within three cycles. Note that this transient time is partly due to the detection and partly due to the transient introduced by the rectifier energization.

VI. Conclusion

A signal processing system for extracting harmonic and reactive current components is presented and its performance when employed in a single-phase active power filter is evaluated. The signal processing system is implemented in Matlab Fixed-Point

Blockset to accommodate the bit-length limitation effects, and interfaced to the power system, which is simulated in PSCAD environment. Investigations show that the proposed method can achieve its steady-state response in about two cycles. Structural robustness of the system allows its implementation with A/D units with as low as 8 bits. Salient features of the system are (1) performance robustness with respect to noise and distortions, (2) insensitivity to the uncertainties of the parameters, (3) frequency-adaptivity and (4) simplicity of the structure.

REFERENCES

[1] J. W. Dixon, J. J. García, and L. Morán, "Control system for three-phase active power filter which simultaneously compensates power factor and unbalance loads," *IEEE Trans. Ind. Electron.*, vol. 42, pp. 636–641, Dec. 1995.

[2] B. N. Singh, A. Chandra, and K. Al-Haddad, "DSP-based indirect-current-controlled STATCOM part 1: evaluation of current control techniques," *Proc. Inst. Elect. Eng., Elect. Power Appl.*, vol. 147, no. 2, pp. 107–112, Mar. 2000.

[3] B. Singh, K. Al-Haddad, and A. Chandra, "A review of active filters for power quality improvement," *IEEE Trans. Ind. Electron.*, vol. 46, pp. 960–971, Oct. 1999.

[4] S. D. Round and D. M. E. Ingram, "An evaluation of techniques for determining active filter compensating currents in unbalanced systems," in *Proc. Eur. Conf. Power Electronics and Applications*, vol. 4, 1997, pp. 767–772.

[5] R. M. Duke and S. D. Round, "The steady-state performance of a controlled current active filter," *IEEE Trans. Power Electron.*, vol. 8, pp. 140–146, Apr. 1993.

[6] J. S. Tepper, J. W. Dixon, G. Venegas, and L. Morán, "A simple frequency-independent method for calculating the reactive and harmonic current in a nonlinear load," *IEEE Trans. Power Electron.*, vol. 43, pp. 647–653, Dec. 1996.

[7] H. Akagi, A. Nabae, and S. Atoh, "Control strategy of active power filters using multiple voltage-source PWM converters," *IEEE Trans. Ind. Applicat.*, vol. IA-22, pp. 460–465, 1986.

[8] T. Tanaka and H. Akagi, "A new method of harmonic power detection based on the instantaneous active power in three-phase circuits," *IEEE Trans. Power Delivery*, vol. 10, pp. 1737–1742, Oct. 1995.

[9] T. E. Nunez-Zuniga and J. A. Pomilio, "Shunt active power filter synthesizing resistive loads," *IEEE Trans. Power Electron.*, vol. 17, pp. 273–278, Mar. 2002.

[10] *Fixed-Point Blockset User's Guide*, MathWorks, Inc., 1995.

[11] *Power Systems Simulation Software Manual*, Manitoba HVDC Research Center.

[12] M. Karimi-Ghartemani and M. R. Iravani, "A nonlinear adaptive filter for on-line signal analysis in power systems: applications," *IEEE Trans. Power Delivery*, vol. 17, pp. 617–622, Apr. 2002.

[13] M. Karimi-Ghartemani and A. K. Ziarani, "Periodic orbit analysis of two dynamical systems for electrical engineering applications," *J. Eng. Math.*, vol. 45, no. 2, pp. 135–154, Feb. 2003.

[14] IEEE Recommended Practices and Requirements for Harmonic Control in Electrical Power Systems, IEEE Std. 519-1992.

[15] M. Sedighy, S. B. Dewsan, and F. P. Dawson, "A robust digital current control method for active power filters," *IEEE Trans. Ind. Applicat.*, vol. 36, pp. 1158–1164, July/Aug. 2000.

Masoud Karimi-Ghartemani received the B.Sc. and M.Sc. degrees in electrical engineering from Isfahan University of Technology, Isfahan, Iran, in 1993 and 1995, respectively. He received the Ph.D. degree in electrical engineering from the University of Toronto, ON, Canada, in 2004.

He was with the Center for Applied Power Electronics (CAPE) in the Department of Electrical and Computer Engineering at the University of Toronto from 1998 to 2001. His research is focused on developing control and signal processing algorithms for power systems protection, control, and power quality.

Hossein Mokhtari received the B.Sc. degree in electrical engineering from Tehran University, Tehran, Iran, in 1989, the M.A.Sc. degree from the University of New Brunswick, Fredericton, NB, Canada, in 1994, and the Ph.D. degree in electrical engineering from the University of Toronto, Toronto, ON, Canada, in 1998.

Currently, he is with the Department of Electrical and Computer engineering at the Sharif University, Tehran, Iran. He was a Consultant Engineer with Electric Power Research Center (EPRC), Tehran.

M. Reza Iravani (M'85–SM'00–F'03) received the B.Sc. degree in electrical engineering from Tehran Polytechnique University, Iran, in 1976, and the M.Sc. and Ph.D. degrees in electrical engineering from the University of Manitoba, Winnipeg, MB, Canada, in 1981 and 1985, respectively.

Currently, he is a Professor at the University of Toronto, ON, Canada. His research interests include power electronics and power system dynamics and control.

Mohammad Sedighy (S'98–M'99) received the B.Sc. degree in electrical engineering from the University of Tehran, Tehran, Iran, in 1990, and the M.A.Sc. and Ph.D. degrees in electrical engineering from the University of Toronto, Toronto, ON, Canada, in 1994 and 1999, respectively.

Currently, he is with Hatch Associates Ltd., Mississauga, ON, Canada. His main areas of interest include application of power electronic converters in power distribution and transmission systems, and power quality assessment and improvement.